Roles of chemokine receptor CX3CR1 in maintaining murine bone homeostasis through the regulation of both osteoblasts and osteoclasts

Akiyoshi Hoshino[1,2,*,‡], Satoshi Ueha[3], Sanshiro Hanada[2], Toshio Imai[4], Masako Ito[5], Kenji Yamamoto[2], Kouji Matsushima[3], Akira Yamaguchi[1,6,‡] and Tadahiro Iimura[1,6,§,‡]

[1]Section of Oral Pathology, Graduate School of Medical and Dental Sciences, Tokyo Medical and Dental University, Tokyo 113-8519, Japan
[2]Vice Director's Lab, Research Institute, National Center for Global Health and Medicine, Tokyo 162-8655, Japan
[3]Department of Molecular Preventive Medicine, Graduate School of Medicine, The University of Tokyo, Tokyo 113-0033, Japan
[4]Kan Research Institute, Inc., Kobe 650-0047, Japan
[5]Department of Radiology, Nagasaki University School of Medicine, Nagasaki 852-8501, Japan
[6]Global Center of Excellence (GCOE) Program, International Research Center for Molecular Science in Tooth and Bone Diseases, Tokyo Medical and Dental University, Tokyo 113-8519, Japan

*Present address: Department of Tumor Pathology, Nagoya University Graduate School of Medicine, Nagoya 466-8501, Japan
[§]Department of Bio-Imaging, Proteoscience Center, Ehime University, Toon 791-0295, Japan
[‡]Authors for correspondence (akira.mpa@tmd.ac.jp; iimura@gcoe.tmd.ac.jp)

Accepted 24 November 2012
Journal of Cell Science 126, 1032–1045

doi: 10.1242/jcs.113910

Summary

Chemokines have recently been reported to be involved in pathological bone destruction. However, the physiological roles of chemokines in bone metabolism *in vivo* have not been well documented. We analyzed the bone phenotypes in *Cx3cr1*-deficient mice. The mice exhibited slight but significant increases in trabecular and cortical thickness, reduced numbers of osteoclasts and increased rates of osteoid formation. Although the morphometric parameters showed marginal differences, the *Cx3cr1*-deficient bones showed an elevated expression of *Osterix/SP7*, which encodes an essential transcriptional factor for osteoblasts, whereas the gene Osteocalcin/*Bglap*, which encodes a late marker, was downregulated. The levels of transcripts for various osteoclastic markers, such as receptor activator of NF-κB (RANK)/TNFRSF11A, receptor activator of NF-κB ligand (RANKL)/TNFSF11, tartrate-resistant acid phosphatase 5b (TRAP5B)/ACP5B, Cathepsin K(CTSK), MMP3 and MMP13, were significantly decreased in the *Cx3cr1*-deficient bones. Cultured *Cx3cr1*-deficient osteoblastic cells showed inverse temporal patterns of osteoblastic marker expression and reduced calcium deposition. Furthermore, *in vitro* studies and immunofluorescence staining against CX3CR1 and CX3CL1 suggested a role for the CX3CR1–CX3CL1 axis in an early stage of osteoblast differentiation, possibly through their trans and cis interactions. Cultured *Cx3cr1*-deficient pre-osteoclasts showed impaired differentiation, mainly due to a deficiency of the $CD115^{+}CD11b^{lo}$ osteoclastogenic population of myeloid-lineage precursors. The treatment of bone-marrow-derived osteoclastic cultures with recombinant CX3CL1 at different time points suggested that the CX3CR1–CX3CL1 axis favors the maintenance of osteoclastic precursors, but not differentiated osteoclasts. These observations uncovered novel roles of the CX3CR1–CX3CL1 axis in the differentiation of both osteoblasts and osteoclasts.

Key words: Chemokines, Chemokine receptors, Osteoclasts, Osteoblasts, Bone remodelling, Bone resorption, Calcification, Bone-coupling factors, Multinucleation, Cell fusion, Osteolysis, Osteopenia

Introduction

Chemokines were originally identified as a group of structurally-related cytokines that direct the homing of circulating leukocytes to sites of inflammation (Charo and Ransohoff, 2006). These ligands bind to cell surface molecules that comprise a group of seven transmembrane Gαi protein-coupled receptors. Chemokines are categorized into four subfamilies according to the arrangement of conserved cysteine residues located in their N-terminal ends: CXC, CC, C and CX3C. In addition to these systematically categorized chemokine families, another related family of chemokine-like factors (CKLF) has been characterized (Han et al., 2001; Han et al., 2003; Wang et al., 2006). CKLF1 is a cytokine with a total of 99 residues, and is a functional ligand for CCR4. It has a CC motif that is identical to that of CCL17 and CCL22, but lacks the additional C-terminus cysteines possessed by other CC chemokines. A group of proteins unrelated structurally to chemokines but having chemokine-like functions, such as HMGB1, macrophage migration inhibitory factor (MIF) and interleukin (IL)-6, is proposed to be named CLF (chemokine-like functions) (Degryse and de Virgilio, 2003; Noels et al., 2009).

Several recent studies have reported that some chemokines are responsible for pathological bone destruction through their regulation of osteoclasts and their precursor cells, which are derived from common progenitor cells in the bone marrow. Some reports have suggested that CCL2 (also called MCP-1) is highly expressed by osteoblasts in response to parathyroid hormone (Li et al., 2007), while its specific receptor, CCR2, has been reported to be involved in postmenopausal bone loss in ovariectomy-induced bone loss models (Binder et al., 2009). In addition, CCL3 (also called MIP-1α), a major proinflammatory chemokine produced at sites of inflammation, stimulates osteoclastogenesis

(Kim et al., 2006; Menu et al., 2006; Oba et al., 2005) and bone resorption in multiple myeloma (Choi et al., 2000; Han et al., 2001; Haringman et al., 2006; Yang et al., 2006), thus indicating it to be a crucial chemokine involved in pathological bone destruction. Another chemokine, CX3CL1 (also called fractalkine), a unique membrane-bound form of chemokine like CXCL16 (Ludwig and Mentlein, 2008; Sheikine and Sirsjö, 2008; Shimaoka et al., 2004; Shimaoka et al., 2007) that exerts dual functions as a chemoattractant and adhesion molecule (Imai et al., 1997), was also reported to be involved in osteoclastogenesis (Koizumi et al., 2009; Saitoh et al., 2007). Although these results suggest that CX3CR1 regulates the differentiation and function of osteoclasts, the roles of CX3CR1 in bone homeostasis are still not fully understood. Such knowledge is crucial for optimizing the treatments targeting chemokines to prevent pathogenic bone resorption. Therefore, it is important to investigate the bone phenotypes in chemokine receptor-deficient mice in order to better understand the physiological roles of chemokines.

We recently demonstrated that *Ccr1*-deficient ($Ccr1^{-/-}$) mice develop osteopenia due to the impaired function of osteoblasts and osteoclasts, which led us to discuss the possibility of using CCR1-related chemokine ligands as therapeutic targets. Bone cells derived from $Ccr1^{-/-}$ mice show diminished expression levels of several chemokine ligands, thus suggesting that hierarchal networks of chemokines participate in bone metabolism (Hoshino et al., 2010). Therefore, in the present study, we investigated the bone features of *Cx3cr1*-deficient mice to further assess the roles of the chemokine receptors in bone metabolism. Both *in vivo* and *in vitro* observations demonstrated the critical roles of the CX3CR1–CX3CL1 axis in maintaining bone homeostasis by regulating the functional differentiation of osteoblasts and osteoclasts, as well as bone cell communication.

Results

The bone phenotypes in *Cx3cr1*-deficient mice suggest possible roles in bone formation, as well as bone resorption

To understand the functions of CX3CR1 in bone metabolism, we first investigated the bone structure of *Cx3cr1*-deficient mice using microCT. The microCT images indicated the presence of slightly increased cancellous trabeculae in the *Cx3cr1*-deficient mice compared to that observed in wild-type mice (Fig. 1A). Quantitative analyses showed slightly elevated parameters of the bone volume per tissue volume (BV/TV), trabecular thickness (Tb.Th.), cortical thickness (Ct.Th.) and trabecular volume (Tb.V.) compared to those observed in wild-type mice, although the trabecular separation (Tb.Sp.) and trabecular number (Tb.N.) did not show significant difference (Fig. 1B). Bone histomorphometric analyses showed higher values of bone volume per tissue volume (BV/TV), osteoid volume (OV/BV), osteoid surface (OS/BS) and bone formation rates (BFR/BS) in the *Cx3cr1*-deficient mice compared to wild-type mice, although the osteoid thickness (O.Th.), osteoblast surface per bone surface (Ob.S/BS), mineral apposition rate (MAR) and the mineralized surface (MS/BS) showed no significant differences between the mice (Fig. 1C). More importantly, the bone histomorphometric analysis showed significant decreases in parameters associated with bone resorption, such as osteoclast numbers (N.Oc./B.Pm) and osteoclast surface areas (Oc.S/BS) (Fig. 1D), which appears to be consistent with a previous report in which anti-CX3CL1 Abs-injected mice exhibited lower scores for the bone resorption index compared to the control IgG-injected mice (Koizumi et al., 2009). Although these parameters of pQCT and from the bone histomorphometric analyses showed marginal differences between wild-type and *Cx3cr1*-deficient mice, they suggested possible roles for *Cx3cr1* in bone formation, as well as in bone resorption.

Impaired expression of osteoblastic and osteoclastic markers in *Cx3cr1*-deficient mice

To investigate the status of osteoblasts and osteoclasts in the bones of *Cx3cr1*-deficient mice, we compared the transcript levels of osteoblast- and osteoclast-related markers in the femurs of wild-type and *Cx3cr1*-deficient mice. Fig. 2A summarizes the changes in the expression levels of transcripts of osteoblast-related markers including transcription factors (Runx2 and Osterix/SP7) (Ducy et al., 1997; Komori et al., 1997; Liu et al., 2001) and bone matrix proteins [Collagen1a1 (Col1a1), Osteonectin (SPARC) and Osteocalcin (BGLAP)]. *Osterix* was significantly upregulated (by ~170%) in the *Cx3cr1*-deficient femurs compared to that observed in the femurs of the wild-type mice, whereas the *Runx2* level was not significantly different. Among the genes encoding bone matrix proteins, *Osteonectin* was significantly upregulated, and *Osteocalcin*, which encodes a marker of mature osteoblasts, was significantly downregulated, in the *Cx3cr1*-deficient mice (Fig. 2A). The expression level of Collagen1a1 did not show any significant differences between the *Cx3cr1*-deficient and wild-type mice (Fig. 2A). These results suggest that *Cx3cr1* regulates both the differentiation and function of osteoblasts.

The expression levels of genes of osteoclasts-related markers, such as *Trap5b/Acp5b* and Cathepsin K (*Ctsk*), were significantly attenuated in the *Cx3cr1*-deficient mice compared to those observed in the wild-type mice (Fig. 2B). The expression levels of *Mmp3* and *Mmp13*, encoding bone-specific matrix metalloproteinases, were also decreased in the *Cx3cr1*-deficient mice (Fig. 2B). Furthermore, the *Cx3cr1*-deficient mice showed significantly decreased serum levels of TRAP5b (Delmas, 1993) and collagen-type I N-telopeptides (NTx) (Schneider and Barrett-Connor, 1997; Takahashi et al., 1997) (Fig. 2C).

Since these results supported the presence of diminished osteoclastic bone resorption in the *Cx3cr1*-deficient mice, we assessed the activation of the RANK–RANKL axis, an essential signaling pathway in the osteoblast–osteoclast interactions that regulates osteoclast differentiation and function. Interestingly, both *Rank/Tnfrsf11a* and *Rankl/Tnfsf11* were significantly downregulated in the *Cx3cr1*-deficient mice compared to the levels observed in wild-type mice (Fig. 2D). Notably, a soluble osteoclastogenesis inhibitory factor gene, Osteoprotegerin (*OPG)/Tnfrsf11b*, was significantly upregulated in the *Cx3cr1*-deficient mice (Fig. 2D), implying that a lack of CX3CR1 impairs osteoclastogenesis through the RANK–RANKL axis.

We further investigated the expression levels of transcripts for CX3CL1, a specific and unique ligand of CX3CR1, CCR1, another chemokine receptor, and its bone-specific ligands, CCL5 and CCL9, in the bones of *Cx3cr1*-deficient mice (Fig. 2E), since we had previously reported critical roles of the CCR1 axis involving CCL5 and CCL9 in the differentiation and function of both osteoblasts and osteoclasts by observing *Ccr1*-deficient mice (Hoshino et al., 2010). Interestingly, the expression of *Cx3cl1*, *Ccr1* and *Ccl9* was almost completely eliminated, and

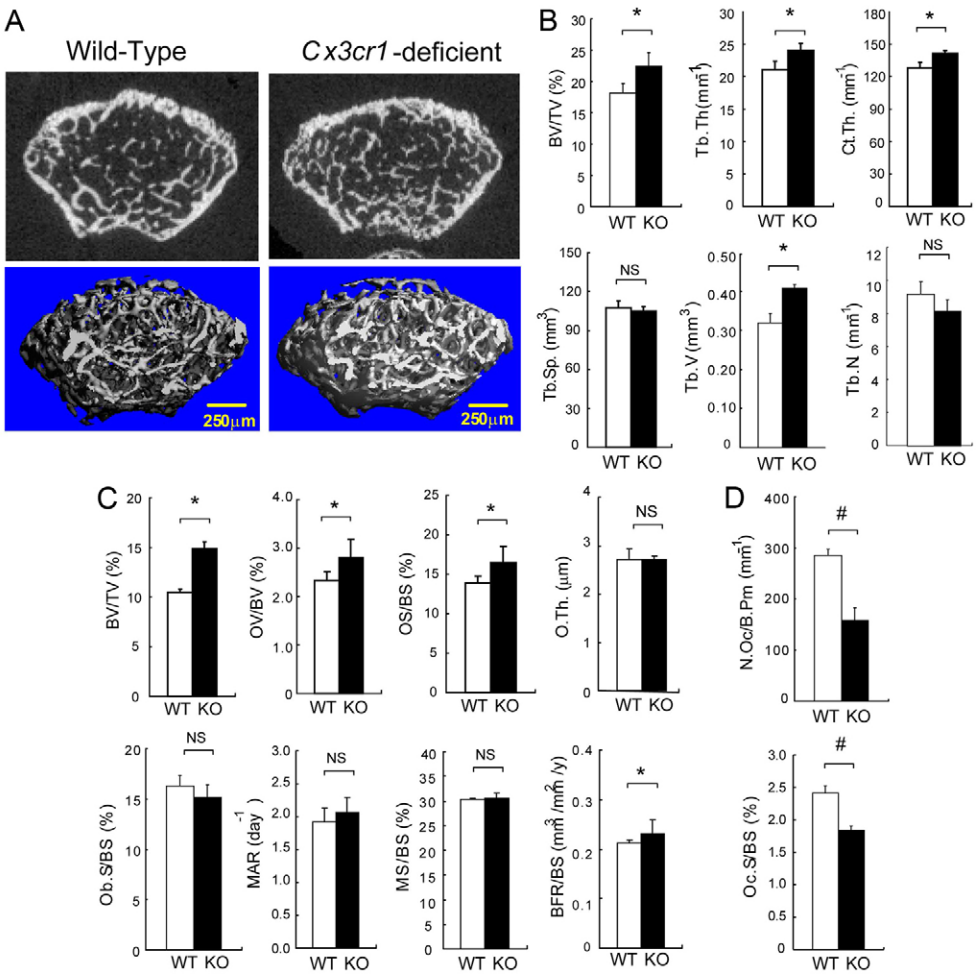

Fig. 1. Immature osteoblasts and reduced numbers of osteoclasts in *Cx3cr1*-deficient mice. (**A**) microCT images of the femurs in wild-type and *Cx3cr1*-deficient mice. (**B**) The bone analyses of distal femurs of wild-type (open bars) and *Cx3cr1*-deficient (filled bars) mice using the microCT analysis in A. Parameters relating to the trabecular structure: bone volume per tissue volume (BV/TV), trabecular thickness (Tb.Th.), cortical bone thickness (Ct.Th.), trabecular separation (Tb.Sp.), trabecular volume (Tb.V.) and trabecular number (Tb.N.). *Significant increases compared to wild-type littermate controls, $P<0.05$. (**C**,**D**) The bone histomorphometric analyses of the distal femurs of wild-type (open bars) and *Cx3cr1*-deficient (filled bars) mice. Parameters relating to trabecular structure and bone formation in C: bone volume per tissue volume (BV/TV), osteoid volume to bone volume (OV/BV), osteoid surface/bone surface (OS/BS), osteoid thickness (O.Th.), osteoblast surface per bone surface (Ob.S/BS), mineral apposition rate (MAR), mineralizing surface per bone surface (MS/BS) and formation rate referenced to the bone surface (BFR/BS). Parameters relating to bone resorption in D: osteoclast number per bone perimeter (N.Oc./B.Pm) and osteoclast surface per bone surface (Oc.S/BS). The bone histomorphometric analysis data are represented as the means ± s.e.m. obtained from eight mice in each group. * and # indicate a significant upregulation and downregulation, respectively ($P<0.05$) from wild-type controls, $P<0.05$.

the level of Ccl5 was significantly downregulated in the bones from *Cx3cr1*-deficient mice (Fig. 2E).

Attenuated differentiation and function in osteoblastic cells isolated from *Cx3cr1*-deficient mice

To elucidate the roles of CX3CR1 in osteoblast differentiation and function, we cultured osteoblastic cells derived from *Cx3cr1*-deficient mice and compared their phenotypes with those from wild-type mice. We first noted that there was significantly reduced calcium deposition (Fig. 3A) in the *Cx3cr1*-deficient osteoblastic cells compared to that observed in the cells of wild-type mice. We next assessed the transcriptional levels of osteoblastic markers using a real-time quantitative PCR (RT-PCR) analysis (Fig. 3B). The temporal expression levels of *Runx2* and *Osterix* in the *Cx3cr1*-deficient cells were inverted compared to those observed in the wild-type cells. On day 14, the *Runx2* expression level was lower, and the *Osterix* expression level was higher, in the *Cx3cr1*-deficient osteoblastic cells than in the cells from the wild-type mice. The *Cx3cr1*-deficient cells showed significantly lower transcription levels of bone-specific alkaline phosphatase (*Balp*)/*Alpl*, Collagen1a1 and Osteonectin on days 0 and 14, and higher levels on day 21, than those observed in the wild-type cells. The Osteocalcin level in the wild-type osteoblasts was dramatically upregulated on day 21; however, its transcription level in the *Cx3cr1*-deficient osteoblastic cells was suppressed throughout the culture period. The temporal expression patterns of the osteoblastic markers suggest that there is a maturation disorder in the *Cx3cr1*-deficient osteoblastic cells.

We next investigated the osteoclast-supporting activities in cultured osteoblastic cells. *Cx3cr1*-deficient osteoblastic cells expressed significantly lower and higher levels of *Rankl* and

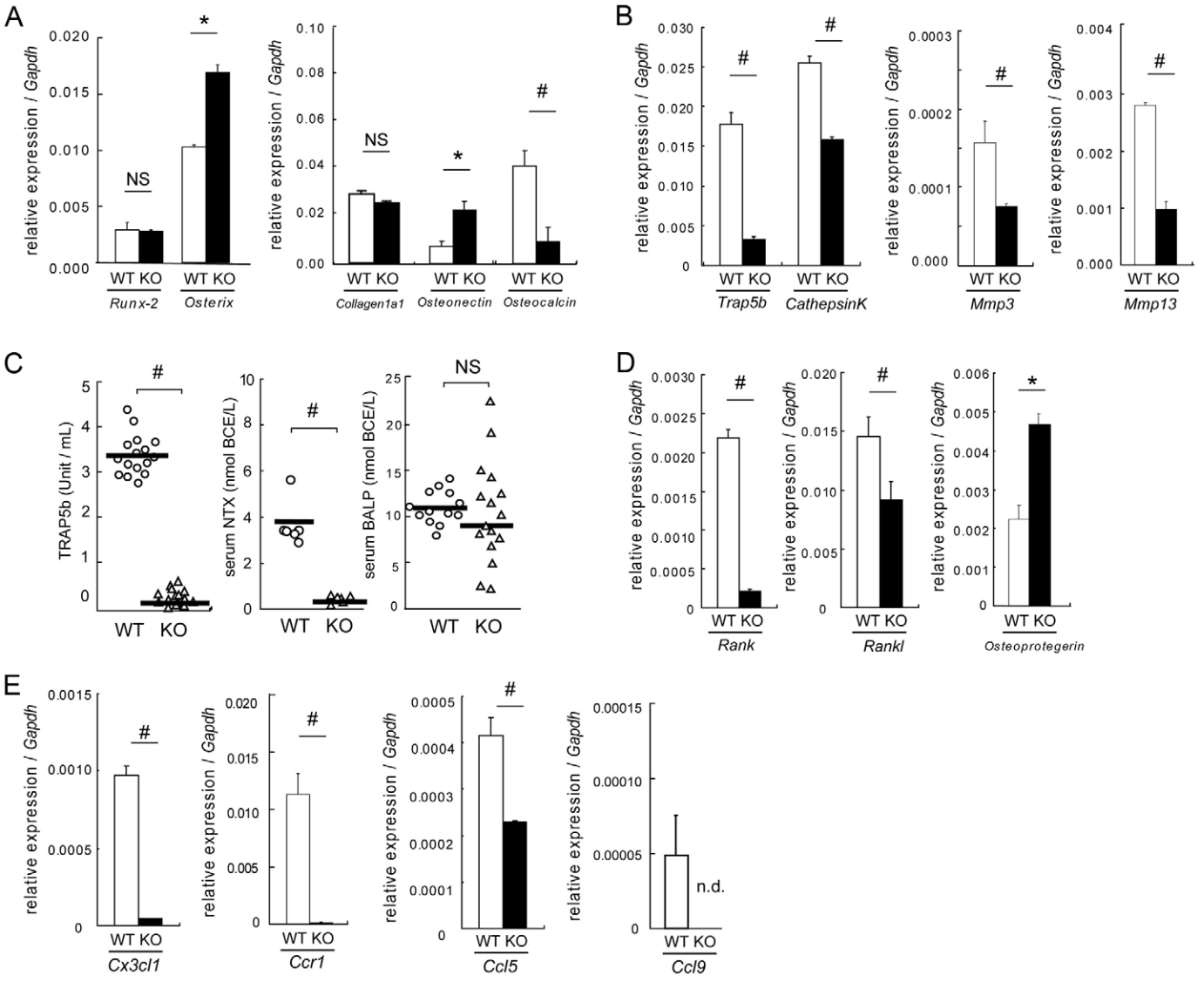

Fig. 2. The expression of genes related to osteoblasts and osteoclasts in *Cx3cr1*-deficient mice. (**A**) Transcripts of osteoblast-related transcription factors (*Runx2* and *Osterix*) and osteoblastic markers (Collagen1a1, Osteonectin and Osteocalcin) extracted from the bone tissue of wild-type (open bars) and *Cx3cr1*-deficient mice (filled bars) were measured using a real-time quantitative PCR (RT-PCR) analysis (mean ± s.e.m., $n=8$). n.d., not detected. (**B**) The expression levels of transcripts of osteolytic markers, bone-resorption enzymes (*Trap5b*, CathepsinK) and bone-related MMPs (*Mmp3* and *Mmp13*) were analyzed using mRNA extracted from bone tissue from wild-type (open bars) and *Cx3cr1*-deficient mice (filled bars). (**C**) The serum levels of TRAP5b (wild-type, $n=10$; *Cx3cr1*-deficient, $n=8$), NTX (wild-type and *Cx3cr1*-deficient, $n=8$) and BALP (wild-type, $n=10$; *Cx3cr1*-deficient, $n=8$) in wild-type (open bars) and *Cx3cr1*-deficient male mice (filled bars) aged 9–13 weeks were measured using ELISAs. Horizontal lines indicate the means. (**D**,**E**) The expression levels of (D) *Rank*, *Rankl* and Osteoprotegerin and (E) specific chemokine of CX3CR1, *Cx3cr1*, chemokine receptor *Ccr1* and chemokines *Ccl5* and *Ccl9*, extracted from the bone tissue of wild-type (open bars) and *Cx3cr1*-deficient (filled bars) mice were measured using a RT-PCR analysis (means ± s.e.m., $n=8$). n.d., not detected.

Osteoprotegerin, respectively, throughout the culture period compared to those observed in wild-type osteoblastic cells (Fig. 3C). This result is consistent with our *in vivo* observations of bone tissue from *Cx3cr1*-deficient mice (as shown in Fig. 2D). We next performed co-cultures of wild-type pre-osteoclasts with osteoblastic cells isolated from either wild-type or *Cx3cr1*-deficient mice. As expected, a significantly reduced number of osteoclasts was formed from the co-cultures with *Cx3cr1*-deficient osteoblastic cells compared to those with wild-type osteoblastic cells (Fig. 3D). Treatment with pertussis toxin (PTX), an inhibitor of Gαi-protein-coupled receptors that is involved in chemokine signaling, prevented the wild-type osteoblastic cells from generating substantial numbers of osteoclasts (Fig. 3C), confirming the requirement of Gαi protein-mediated signal for osteoclastgenesis as previously reported (Hoshino et al., 2010).

We then investigated the transcript expression levels of CX3CR1, its unique ligand, CX3CL1, and another chemokine receptor, CCR1, in osteoblastic cell cultures (Fig. 3E). The temporal expression patterns showed that the level of *Cx3cr1* transcription on days 0 and 14 was significantly higher than that on day 21, suggesting that there was downregulation of the *Cx3cr1* transcript depending on the maturation of osteoblasts. The level of *Cx3cl1* was greatly upregulated on day 14 only in the

wild-type osteoblastic cells. In contrast, the level of *Cx3cl1* in *Cx3cr1*-deficient osteoblastic cells was dramatically suppressed, and was maintained at the basal level throughout the culture period. These temporal patterns of *Cx3cr1* and *Cx3cl1* expression suggest that the interaction between the receptor and the ligand likely occurs at an early stage of osteoblast differentiation, but not a late stage of mineralization.

The transcriptional level of *Ccr1* was significantly downregulated throughout the culture period in *Cx3cr1*-deficient mice compared to that observed in wild-type mice. The secretion of CCL5 and CCL9, critical ligands for CCR1 required for osteoblast differentiation (Hoshino et al., 2010), were also significantly reduced in *Cx3cr1*-deficient osteoblastic cells (Fig. 3F). These findings suggest that osteoblastic phenotypes in *Cx3cr1*-deficient mice involve the reduced function of the CCR1 axis.

Predominant expression of CX3CR1 and CX3CL1 proteins in osteoblasts in trabecular bone compared to those in lining cells on the cortical bone surface

The *in vivo* expression of the CX3CR1 and CX3CL1 proteins in osteoblasts was investigated by immunofluorescence using antibodies specific for the proteins in tissue sections of tibiae from 4-week-old mice. Specific signals against CX3CR1 and CX3CL1 were predominantly detected in the cuboidal osteoblasts covering primary trabeculae adjacent to the growth plate cartilage (Fig. 4A, upper panels). In the mid-shaft region, faint signals for these proteins were observed in the cells lining the endosteum on the cortical bone surface (Fig. 4A, lower panels, indicated by arrowheads), while intense signals were detected in bone marrow cells.

We next carried out the same immunofluorescence studies on MC3T3-El osteoblastic cells to investigate their subcellular localizations in these cells. Double labeling of the CX3CR1 and CX3CL1 proteins demonstrated that both proteins were mostly colocalized in the cytoplasm and surface of the cells in the pre-confluent state (Fig. 4B, upper panels). Interestingly, they were also detected in the cellular processes that connected cells to each other. However, in sub-confluent state, only a few cells showed intense signals for CX3CR1 and CX3CL1, while most of the cells exhibited very faint signals (Fig. 4B, lower panels). These observations were consistent with the temporal expression patterns of *Cx3cr1* and *Cx3cl1* in osteoblastic cell cultures derived from bones (Fig. 3E), thus suggesting that their interaction occurs during an early stage of osteoblast differentiation.

Recombinant CX3CL1 stimulates the expression of osteoblastic transcriptional factors

To further investigate the roles of the CX3CL1–CX3CR1 axis, we inoculated the soluble form of recombinant mouse CX3CL1 (rmCX3CL1) into the primary osteoblastic cell cultures from wild-type bones and observed its effects on the expression of bone markers by RT-PCR (Fig. 5). The rmCX3CL1 strongly stimulated the expression of *Runx2* and *Osterix* in a dose-dependent manner. The Collagen1a1 level was significantly stimulated by 50 ng/ml rmCX3CL1, but was downregulated by a higher dose (100 ng/ml). Only the highest dose of rmCX3CL1 (100 ng/ml) significantly inhibited the expression of *Balp*, Osteopontin/*Spp1* and Osteocalcin. The endogenous *Cx3cl1* expression was dose-dependently downregulated, while the *Rankl* level was not significantly affected by rmCX3CL1. Therefore, CX3CL1 stimulates the expression of transcription factors that are essential for osteoblastogenesis and the early function of osteoblasts.

Impaired osteoclast differentiation and bone-resorbing activity in osteoclastic cells isolated from CX3CR1-deficient mice

To further corroborate the necessity of CX3CR1 in osteoclast differentiation and function, we employed *in vitro* osteoclast culture systems induced from myeloid precursors in the presence of M-CSF and RANKL. We first undertook a morphological examination of osteoclastogenesis in *Cx3cr1*-deficient osteoclast precursors. The fluorescent staining of F-actin in cultured osteoclasts showed no obvious morphological differences in actin ring formation between the wild-type and *Cx3cr1*-deficient cells (Fig. 6A, in green). However, there was no detectable staining for Cathepsin K in *Cx3cr1*-deficient osteoclasts, whereas wild-type cells showed positive signals in mononuclear osteoclast progenitors and multinucleated osteoclastic cells (Fig. 6A, in red). Fig. 6B summarizes the expression levels of osteoclast-related markers as determined by RT-PCR. The expression levels of *Rank*, *Nfat-c1*, *Trap5b*, Cathepsin K, Integrin alphaV (*ItgaV*) and Integrin beta3 (*Itgb3*) in *Cx3cr1*-deficient cells were significantly lower compared to those observed in wild-type cells. In contrast, the expression levels of myeloid-lineage markers, such as $S1P_1$ (Ishii et al., 2009) and *Irf-8* (Zhao et al., 2009) in the *Cx3cr1*-deficient osteoclasts were increased compared to those observed in wild-type cells. In addition, a pit formation assay performed using bone slices demonstrated that wild-type osteoclasts completely resorb both mineralized and unmineralized bone matrices, while *Cx3cr1*-deficient osteoclasts fail to remove unmineralized bone matrices (Fig. 6C). We therefore conducted a collagen-based zymography study to assess the collagenolytic activity of the osteoclastic cells. This study revealed that the lysates of *Cx3cr1*-deficient osteoclasts does not fully digest type-I collagens (Fig. 6D).

Impaired expression of the CCR1 axis in *Cx3cr1*-deficient osteoclasts

We further investigated whether changes in the CCR1 axis were involved in the *Cx3cr1*-deficient osteoclast differentiation. First, the time course changes in the expression levels of *Cx3cr1* and *Ccr1* during the culture period were assessed using wild-type osteoclast precursors (Fig. 7A). The expression level of *Cx3cr1* on day 0 was ~10 times higher than that of *Ccr1*. The *Cx3cr1* expression was rapidly downregulated on day 4, and then was subsequently sustained at a lower level. The transcriptional level of *Ccr1* showed a peak on day 4. These results suggest that the expression levels of *Cx3cr1* and *Ccr1* change depending on the osteoclast maturation stages: a high expression level of *Cx3cr1* is observed at an early stage of osteoclastogenesis, while an increased level of *Ccr1* is observed during the middle to later stages.

We next compared the expression levels of *Ccr1*, *Ccl5* and *Ccl9* between *Cx3cr1*-deficient and wild-type osteoclasts, since they are a critical chemokine receptor and its ligands are required for osteoclast differentiation (Hoshino et al., 2010). The expression levels of *Ccr1* and *Ccl5* in the *Cx3cr1*-deficient osteoclasts were significantly downregulated compared to those observed in wild-type mouse-derived osteoclasts, whereas the

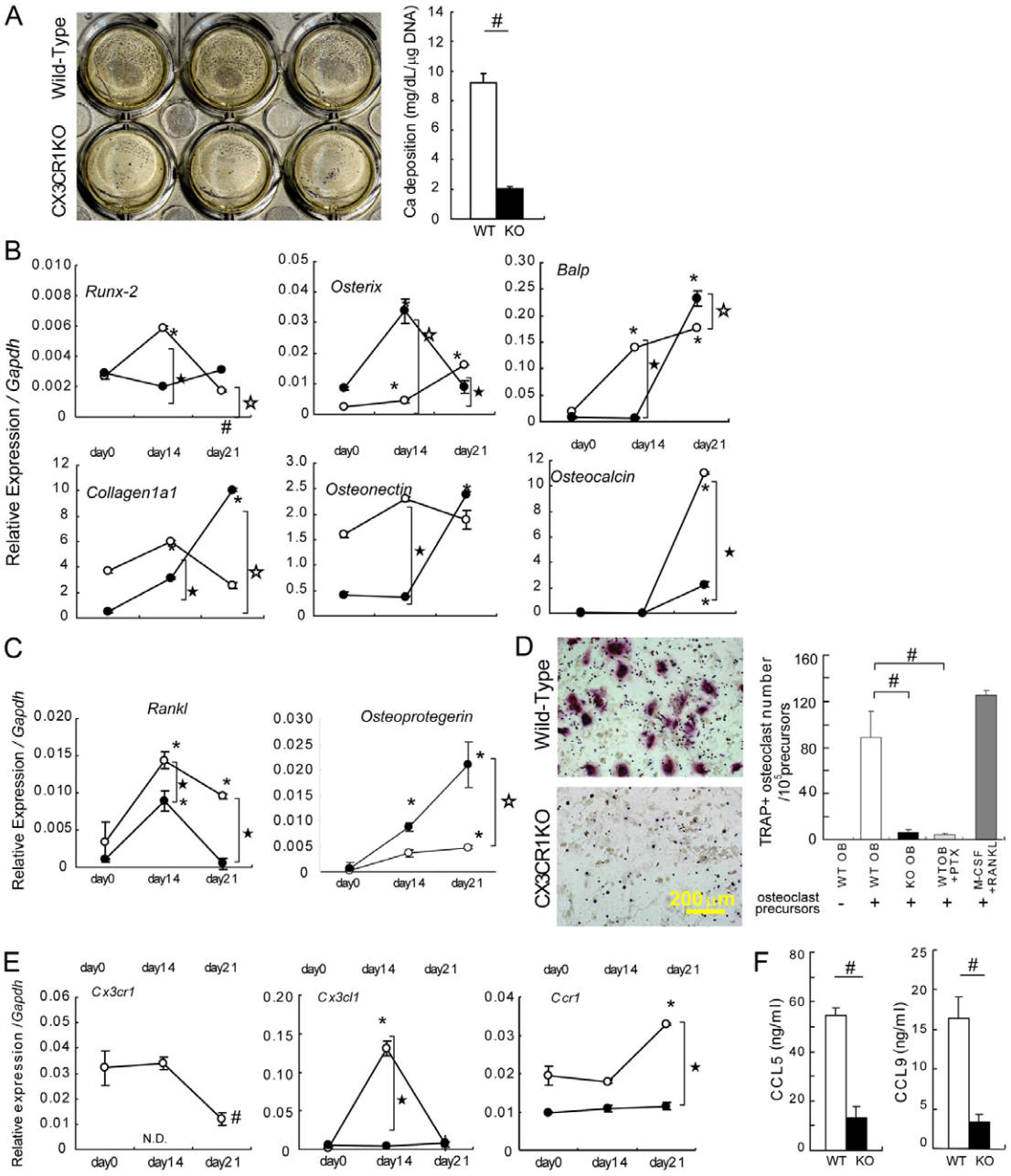

Fig. 3. Impairment of osteoblast differentiation in *CX3CR1*-deficient cells. (**A**) Osteoblastic cells isolated from wild-type (open bars) and *Cx3cr1*-deficient mice (filled bars) were cultured. The mineralized nodules were stained using von Kossa's method and the samples were photographed. The number of mineralized nodules was calculated (means ± s.e.m., $n=4$), and the calcium content in the nodules was measured and normalized to the DNA content in the lysates (means ± s.e.m., $n=4$; right graph). (**B**) The relative expression levels of transcripts of osteoblastic transcription factors (*Runx2* and *Osterix*) and markers (*Balp*, Collagen1a1, Osteonectin and Osteocalcin) by immature (day 14, before mineral deposition) or mature (day 21, with mineralization) osteoblastic cells isolated from wild-type (open circle) and *Cx3cr1*-deficient mice (filled circle) were measured using RT-PCR (means ± s.e.m. $n=8$). The statistical significance was determined with the Tukey–Kramer HSD test. * and # indicate a significant upregulation and downregulation, respectively ($P<0.05$) compared with unstimulated stromal cells ($P<0.05$). There were significant differences between wild-type and *Cx3cr1*-deficient cells, with significant upregulation denoted by ☆ and downregulation by ★, respectively ($P<0.05$). (**C**,**D**) Co-culture of osteoblasts and osteoclasts from wild-type and *Cx3cr1*-deficient mice. (C) The relative expression levels of *Rankl* and Osteoprotegerin by the osteoblastic cells derived from wild-type (open circles) and *Cx3cr1*-deficient mice (filled circles) were measured using RT-PCR (means ± s.e.m., $n=8$). (D) Osteoclasts were induced from wild-type osteoclast precursors by co-culture with osteoblasts of wild-type and *Cx3cr1*-deficient mice. (Left panels) Multinuclear osteoclasts were visualized with TRAP chromogenic stain on osteoblastic cells derived from wild-type and *Cx3cr1*-deficient mice (magnification ×100). (Right panel) The number of $TRAP^+$ multinuclear osteoclasts was counted (means ± s.e.m., from duplicate experiments, $n=3$). Osteoclast culture with M-CSF and RANKL without osteoblasts were carried out as positive controls. #Significant differences from the co-culture of osteoclasts with wild-type osteoblasts, $P<0.05$. (**E**) The relative expression levels of *Cx3cr1*, *Cx3cl1* and *Ccr1* by the immature and mature osteoblastic cells from wild-type (open circles) and *Cx3cr1*-deficient mice (filled circles) as measured by RT-PCR (means ± s.e.m., $n=6$). The difference between the wild-type and *Cx3cr1*-deficient cells was statistically significant [downregulation (★), N.D. not detected]. (**F**) Chemokines (CCL5 and CCL9) in the culture supernatants of wild-type and *Cx3cr1*-deficient osteoblastic cells were measured using ELISAs (means ± s.e.m., duplicated, $n=4$).

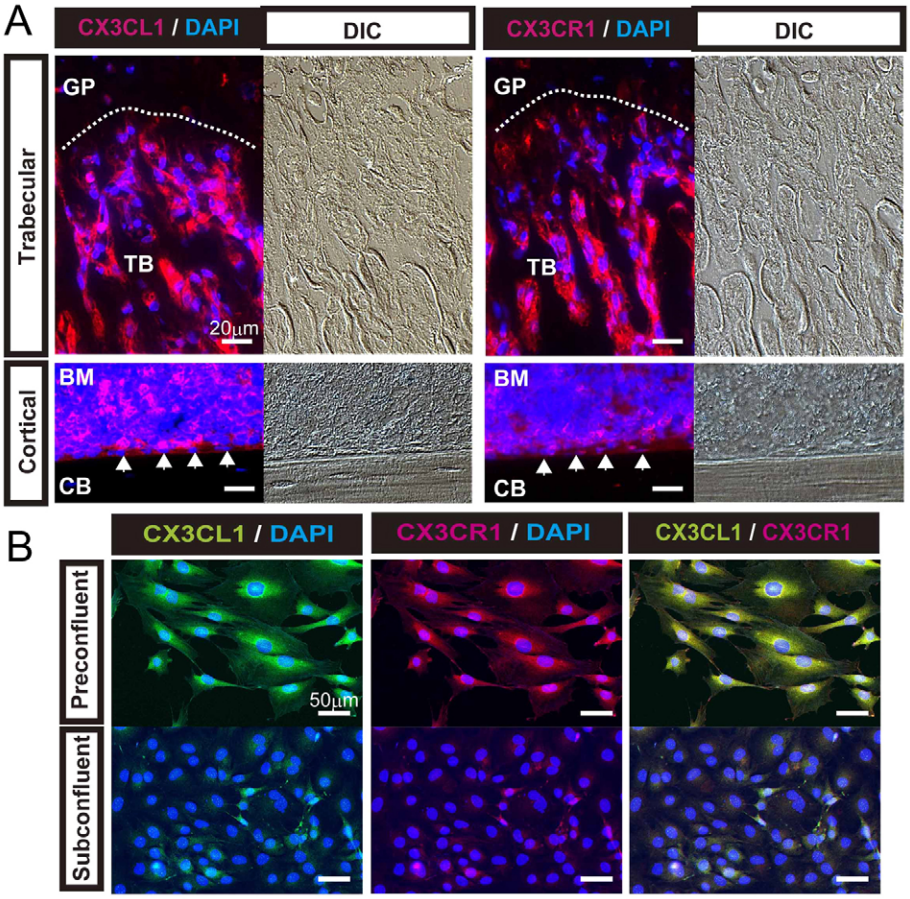

Fig. 4. The expression of CX3CR1 and CX3CL1 proteins in osteoblasts *in vivo* and *in vitro*. (**A**) Immunofluorescence studies using specific antibodies against CX3CR1 and CX3CL1 were carried out on sections of tibiae from 4-week-old mice. CX3CR1 and CX3CL1 were detected by secondary antibodies conjugated with Alexa Fluor 568 (in red). Sections were counterstained with DAPI to detect nuclei (in blue). Differential interference contrast (DIC) images of each section were obtained for morphological observation. Scale bars: 20 μm. The dotted lines demarcate the border between the growth plate (GP) cartilage and primary trabeculae (TB). The arrows indicate endosteum lining cells. BM, bone marrow; CB, cortical bone. (**B**) Double immunostaining for CX3CR1 and CX3CL1 was carried out on MC3T3-E1 cells. CX3CR1 and CX3CL1 were detected by secondary antibodies conjugated with Alexa Fluor 568 (in red) and 488 (in green), respectively. Sections were counterstained with DAPI to detect nuclei (in blue). Merged images are shown in the right panels. Scale bars: 50 μm.

Ccl9 expression in *Cx3cr1*-deficient osteoclasts was significantly upregulated (Fig. 7B). These changes in chemokine ligand expression were consistently confirmed at the protein levels in the media from cultured cells (Fig. 7C).

Population changes in osteoclastic precursors associated with CX3CR1 deficiency after RANKL simulation

We examined whether CX3CR1 deficiency affects the population changes in RANK-expressing osteoclast precursors (Fig. 7D). After the culture of bone-marrow-derived cells with M-CSF and RANKL, the cellular profiles of osteoclast precursors were analyzed using a flow cytometric analysis. This analysis revealed that *Cx3cr1*-deficient mice have slightly higher numbers of $CD11b^{+}CD115^{+}$ myeloid-lineage precursors compared to wild-type mice (14.35±1.90% in *Cx3cr1*-deficient mice to 13.40±0.95% in wild-type mice; Fig. 7D; Table 1). However, the subpopulations of osteoclast precursors (R2-gated cells), which express $CD11b^{lo}RANK^{dull}$ and are reported to be required for multi-nuclear osteoclasts (Arai et al., 1999; Hoshino et al., 2010), were significantly reduced in *Cx3cr1*-deficient cells (1.01±0.02% in *Cx3cr1*-deficient mice to 1.89±0.55% in wild-type mice). In addition, the expression level of RANK in the R2-gated ($CD11b^{lo}$) cells was diminished in *Cx3cr1*-deficient cells. The population changes in these osteoclastogenic subpopulations likely contribute to the reduced expression of osteoclast markers in *Cx3cr1*-deficient osteoclastic cells, as observed in *Ccr1*-deficient osteoclastic cells (Hoshino et al., 2010).

Treatment with recombinant CX3CL1 prior to, but not after, RANKL stimulation delays osteoclastic marker expression

To dissociate the temporal roles of the CX3CR1–CX3CL1 axis in osteoclast differentiation *in vitro*, we treated the bone-marrow-derived osteoclast cultures stimulated by M-CFS and RANKL with rmCX3CL1 at two distinct time points, and analyzed the time-dependent expression levels of osteoclast and myeloid lineage markers by RT-PCR (Fig. 8). Since we noticed that the expression of *Cx3cr1* was readily downregulated within 6 hours after RANKL inoculation (Fig. 8A and data not shown), we treated the bone-marrow-derived osteoclast precursors with rmCX3CL1 1 hour prior to RANKL stimulation on day 1. Accordingly, when rmCX3CL1 was inoculated on day 1, the activation of osteoclastic marker genes such as *Rank*, *Nfat-c1*, *Trap* and Cathepsin K was delayed compared to those in cells treated with the control vehicle, whereas the expression of myeloid-lineage marker genes, such as $S1P_1$ and *Irf8*, was sustained at higher levels than those in the control (Fig. 8A). Consistently, a time-dependent downregulation of the *Cx3cr1* level observed in control cells, and was delayed in the treated cells. The expression of *Ccr1* in the treated cells was sustained at a low level, while it was upregulated in control. However, the treatment with rmCX3CL1 initiated on day 4 after RANKL stimulation did not lead to any obvious differences between the treated and control cells in terms of their temporal expression patterns of these markers and chemokine receptors (Fig. 8B).

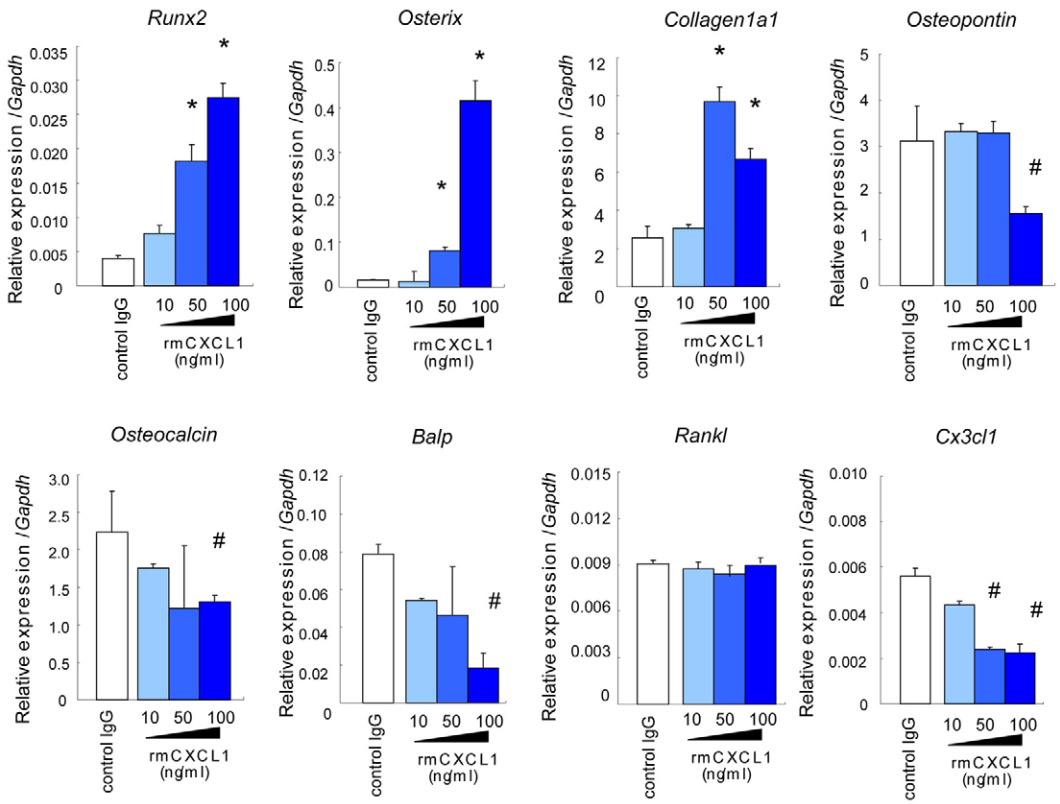

Fig. 5. Enhancement of *Runx2* and *Osterix* expression by treatment with recombinant CX3CL1 in a dose-dependent manner. The relative expression levels of osteoblastic markers and *Cx3cl1* in wild-type osteoblasts treated with rmCX3CL1 (10, 50 and 100 ng/ml) were determined by RT-PCR. The data were compared with the wild-type osteoblasts stimulated with control vehicle (means ± s.e.m., $n=3$). The statistical significance was determined by the Tukey–Kramer HSD test. * and # indicate a significant upregulation and downregulation, respectively ($P<0.05$) between control and rmCX3CL1 stimulation.

Discussion

The roles of the CX3CR1–CX3CL1 axis in osteoblast differentiation

The results of our bone histomorphometric study indicated that there was impaired osteoblast differentiation and function in *Cx3cr1*-deficient mice (Fig. 1C). Since the roles of the CX3CR1–CX3CL1 axis in osteoblast differentiation have not been fully documented, we further investigated the functional role of the CX3CR1–CX3CL1 axis in osteoblast differentiation. Immunofluorescence staining for CX3CR1 and CX3CL1 on bone specimens revealed that these two proteins were expressed predominantly in the cuboidal cells covering trabecular bone, while faint signals were detected in the flat lining cells on the surface of the cortical bone of the diaphysis. Our previous work demonstrated that the cuboidal cells covering trabecular bone exhibited active beta-catenin signaling and *Osterix* expression, which are associated with active osteoblast formation and an early stage of osteoblast function (Watanabe et al., 2012). In cultured osteoblastic MC3T3-E1 cells, CX3CR1 and CX3CL1 were detectable in the cytoplasm and cellular processes in their pre-confluent state; however, they appeared to be downregulated in their sub-confluent state and in later stages. These findings, together with the temporal expression patterns of *Cx3cr1* and *Cx3cl1* observed during cultured osteoblast differentiation (Fig. 3E), suggest that the CX3CR1–CX3CL1 axis plays a role in an early stage of osteoblast differentiation. Furthermore, the subcellular localization of these two proteins suggests possible cis and trans interactions between CX3CL1 and CX3CR1 in osteoblasts.

The cultured osteoblastic cells isolated from *Cx3cr1*-deficient mice also showed complicated changes in the temporal expression patterns of osteoblastic markers, and decreased calcium deposition (Fig. 3A,B). *Runx2* and *Osterix* encode essential transcription factors for osteoblast commitment and differentiation at an early stage (Kanatani et al., 2006; Komori et al., 1997; Liu et al., 2001; Nakashima et al., 2002). Recently, Yoshida et al. reported that sustained expression of *Osterix* and *Runx2* inhibited osteoblast differentiation from proceeding to a late stage in a reciprocally independent manner (Yoshida et al., 2012). Therefore, it is possible that the inverse temporal downregulation and upregulation of transcription factors such as *Runx2* and *Osterix,* as was observed *in vitro* (Fig. 3B), may cause spatiotemporally disordered bone matrix deposition that eventually results in impaired mineral deposition, which may contribute to the increased osteoid volume in the bones of *Cx3cr1*-deficient mice (Fig. 1C). Treatment of wild-type mouse-derived osteoblastic cultures with rmCX3CL1 stimulated the expression of *Runx2* and *Osterix*, but had inhibitory effects on the expression of bone matrix proteins (Fig. 5). Taken together, these findings suggest that the CX3CR1–CX3CL1 axis plays important roles favoring an early stage of osteoblast differentiation, and thus contribute to the regulation of its proper functional maturation.

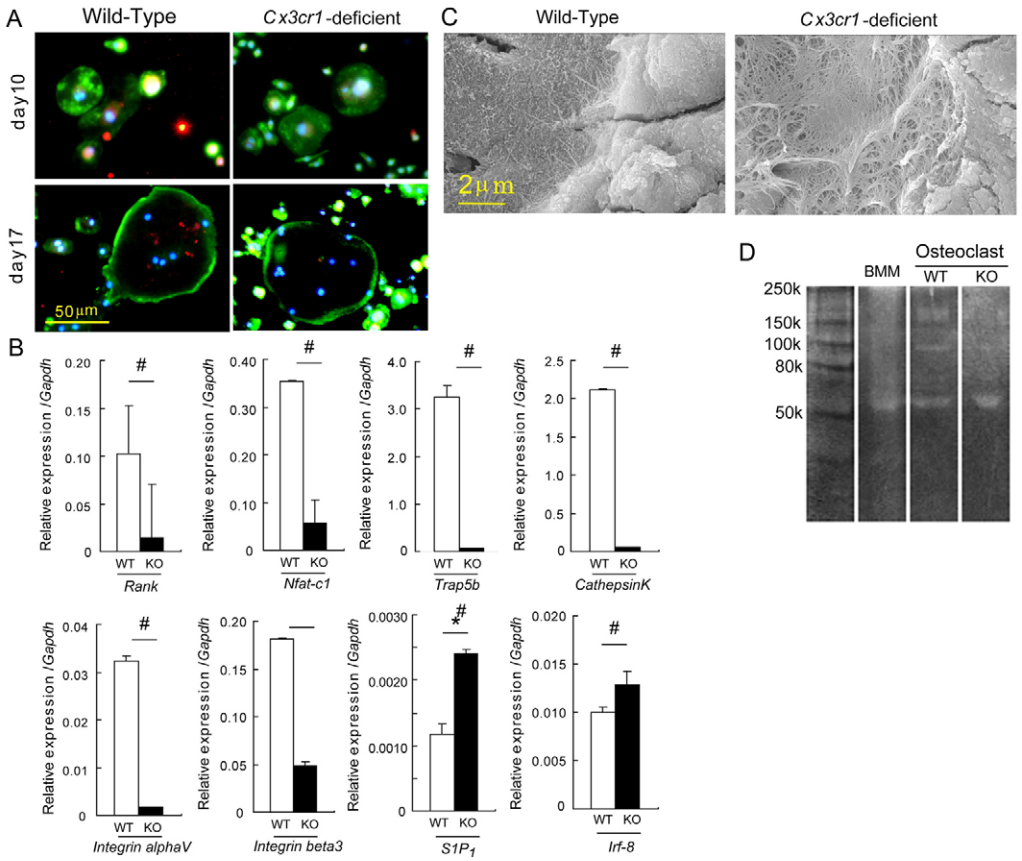

Fig. 6. Impairment of osteoclast functions by CX3CR1 deficiency. (**A**), Osteoclastic cells were induced from the bone marrow of wild-type and *Cx3cr1*-deficient mice using M-CSF and RANKL treatment. *In vitro* osteoclast cultures from wild-type and *Cx3cr1*-deficient precursors were carried out for 10 days (upper panels) or 17 days (lower panels) and cultures were stained with an anti-CathepsinK polyclonal antibody (red), and for F-actin (green) and nuclei (blue). Scale bar: 50 μm. (**B**) The relative expression levels of transcripts of osteoclastic differentiation markers on day 4 after culture[RANK and its downstream transcription factor NFATC1; bone-specific enzymes, TRAP5B and CathepsinK protease; osteoclast-specific integrins alphaV and beta3; and myeloid-lineage cell markers $S1P_1$ and IRF-8] in wild-type (open bars) and *Cx3cr1*-deficient (filled bars) preosteoclasts were measured by RT-PCR (means ± s.e.m., $n=5$). *Significantly upregulated, #significantly downregulated compared with wild-type controls, $P<0.05$. (**C**) Scanning electron micrographs of the pit formation assay of wild-type and *Cx3cr1*-deficient osteoclasts. Scale bar: 2 μm. (**D**) The collagen digestion activity of wild-type and *Cx3cr1*-deficient osteoclasts was measured using collagen-based zymography. BMM, cell lysates from bone-marrow-derived macrophages (10 μg protein/lane); WT and KO, wild-type and *Cx3cr1*-deficient osteoclast lysates (1 and 10 μg protein/lane), respectively.

We also observed a significant suppression of *Ccr1* in osteoblastic cells isolated from *Cx3cr1*-deficient mice throughout the culture period (Fig. 3E). As we previously observed in $Ccr1^{-/-}$ osteoblastic cells, the levels of chemokine ligands for CCR1, such as CCL5 and CCL9, were significantly reduced in *Cx3cr1*-deficient osteoblastic cells (Fig. 3F). These findings suggest that CX3CR1 acts upstream of CCR1 in a chemokine-dependent amplification loop that sustains or amplifies the chemokine signaling networks involved in osteoblast differentiation, as we previously discussed (Hoshino et al., 2010). Indeed, we observed differences in the temporal expression patterns of *Cx3cr1* and *Ccr1*, wherein *Cx3cr1* was upregulated at an early stage and the *Ccr1* expression was augmented in a later stage in wild-type osteoblastic cell cultures (Fig. 3E). Therefore, one possible reason for the complex phenotypes of bone formation and osteoblastic dysfunction associated with CX3CR1 deficiency is that the chemokine networks impaired by the loss of CX3CR1 cause changes in the spatiotemporal inputs of chemokine signaling to osteoblastic cells, which may lead to the temporally disordered expression of osteogenic transcription factors and bone matrix proteins, thus resulting in impaired mineral deposition.

The roles of the CX3CR1–CX3CL1 axis in the maintenance of osteoclast precursors

The osteoclast dysfunction resulting from CX3CR1 deficiency could be largely associated with diminished signaling along the RANK–RANKL axis. The downregulation of both *Rank* and *Rankl*, and the upregulation of Osteoprotegerin, were observed in the bone tissue of *Cx3cr1*-deficient mice (Fig. 2D).

Cultured osteoblastic cells isolated from *Cx3cr1*-deficient mice exhibited remarkable reductions in the *Rankl* expression level (Fig. 3C). Co-cultures of wild-type pre-osteoclasts with osteoblastic cells from *Cx3cr1*-deficient mice failed to induce TRAP-positive osteoclasts (Fig. 3C), confirming the presence of a functional reduction in the osteoclast-supporting activity in *Cx3cr1*-deficient osteoblastic cells, most likely due to the downregulation of *Rankl*. Furthermore, in *Cx3cr1*-deficient osteoclasts, the levels of *Rank* and other osteoclastic markers were decreased, while the levels of myeloid-lineage markers

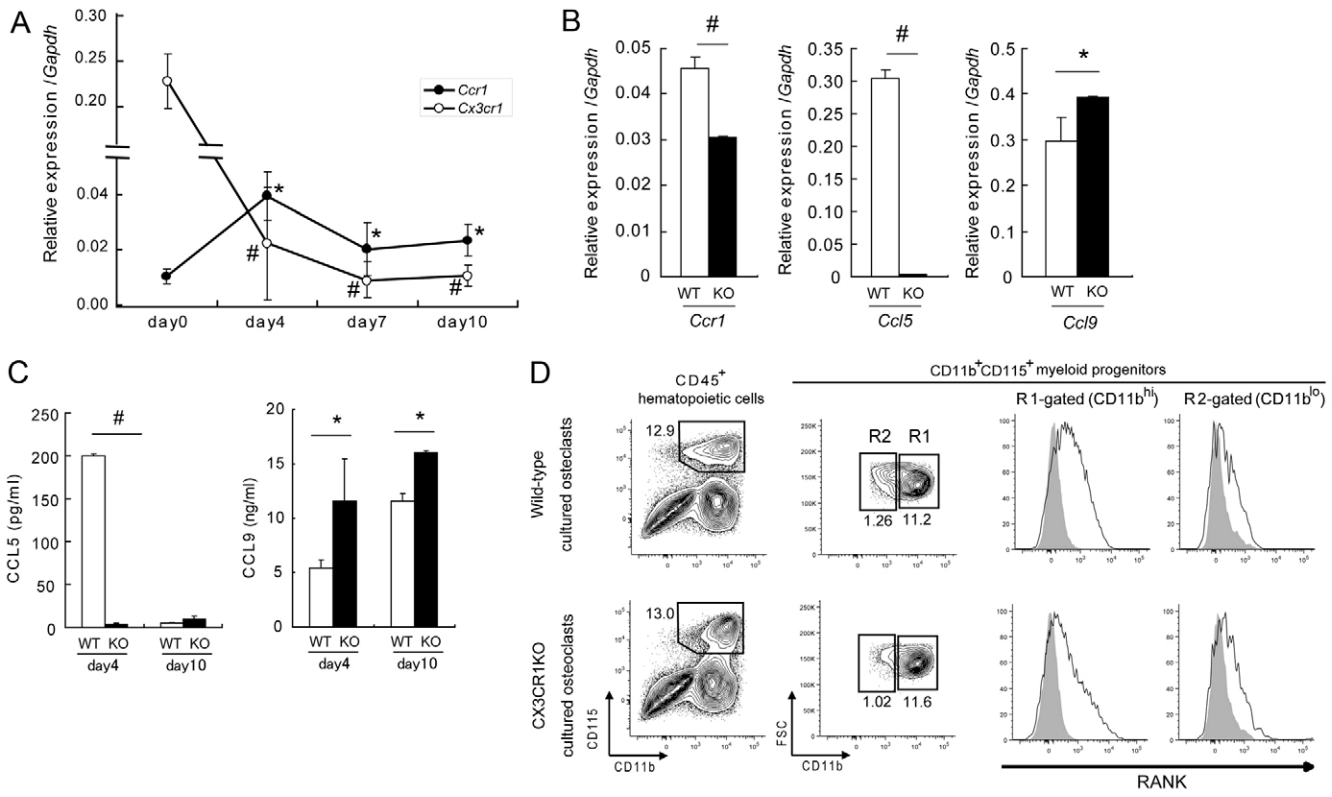

Fig. 7. Changes in the CCR1-mediated axis and the osteoclasic precursor population caused by CX3CR1 deficiency. (**A**) The temporal expression profiles of chemokine receptors *Ccr1* and *Cx3cr1* by wild-type precursors were measured using RT-PCR (means ± s.d., $n=5$). The levels are normalized to the expression of *Gapdh*. * and # indicate significant upregulation and downregulation, respectively, compared with the levels on day 0 ($P<0.05$). Osteoclastic cells were induced from the bone marrow of wild-type and *Cx3cr1*-deficient mice by treatment with M-CSF and RANKL. (**B**) The expression levels of transcripts of the chemokine receptor CCR1 and bone-related chemokines (CCL9 and CCL5) extracted from osteoclastic cells of wild-type (open bars) and *Cx3cr1*-deficient mice (filled bars) were measured using a RT-PCR (means ± s.e.m., $n=8$). n.d., not detected. (**C**) Endogenous CCL5 and CCL9 in the culture supernatant of wild-type (open bars) and *Cx3cr1*-deficient osteoclastic (filled bars) cells were measured using ELISAs (means ± s.e.m., experiments performed in duplicate, $n=3$). (**D**) A population analysis of RANK in $CD45^+CD11b^+CD115^+$ osteoclastic precursors isolated from the bone marrow of wild-type and *Cx3cr1*-deficient mice after 4 days in culture was analyzed by flow cytometry. Histograms were gated on the $CD11b^{hi}RANK^+$ (R1-gated) subpopulation and $CD11b^{lo}RANK^{dull}$ (R2-gated) subpopulation of $CD11b^+CD115^+$ osteoclastic precursors. The surface expression levels of RANK (bold line) are overlaid on cells stained with subclass-matched control IgG (shaded histogram). Plots and histograms are shown as the representative data of three independent experiments, and the population ratio is shown as the mean percentage ± s.e.m. ($n=3$).

were increased (Fig. 6B). These differences in the expression of various markers and functions in *Cx3cr1*-deficient osteoclasts compared to those in wild-type cells could be due to functional changes in the differentiation potential of these cells prior to the culture. Given that no detectable level of *Cx3cl1* was expressed in the osteoclast lineage cells (Koizumi et al., 2009) and that the expression of *Cx3cr1* in wild-type mouse-derived osteoclastic cells was readily downregulated to the basal level after RANKL stimulation (Fig. 5A), the physiological interaction between CX3CL1 and CX3CR1 possibly occurs prior to, and/or concomitantly with, the initial RANK–RANKL interaction to induce osteoclastogenesis in the bone marrow environment where other type of cells, such as endothelial cells and osteoblastic cells, express CX3CL1 (Bazan et al., 1997; Koizumi et al., 2009). Indeed, our flow cytometric analysis of bone marrow cells after M-CSF and RANKL stimulation demonstrated that there was a slight increase in the number of myeloid precursors, but a significant decrease in osteoclastic precursors (R2 gated cells) with lower RANK expression in *Cx3cr1*-deficient cells (Fig. 7D; Table 1), strongly suggesting a critical role for *Cx3cl1* in the regulation of osteoclast precursor populations.

Consistent with these ideas regarding the roles of the CX3CR1–CX3CL1 axis in the osteoclast precursor and immature osteoclast stages, treatment of the osteoclastic cells with rmCX3CL1 prior to RANKL stimulation led to significant downregulation of osteoclastic markers, while the myeloid-lineage markers were upregulated (Fig. 8A**)**. However, no obvious changes in either osteoclastic or myeloid-lineage markers were observed when this treatment was performed after RANKL stimulation on day 4 (Fig. 8B). These findings regarding the distinct timing of CX3CL1 treatment suggest a role for the CX3CR1–CX3CL1 axis in sustaining osteoclastic precursors, with a smaller contribution to the differentiation of mature osteoclasts. Collectively, our current findings suggest that the CX3CR1–CX3CL1 axis plays a relevant role in the maintenance of osteoclastic precursors, which may have favorable roles in the initial attraction and the subsequent adhesion of osteoclast precursors by osteoblasts in the bone

Table 1. Population analysis of RANK in CD45$^+$CD11b$^+$CD115$^+$ osteoclastic precursors of wild-type, *Ccr1*-deficient and *Cx3cr1*-deficient mice

	CD45$^+$ (%)	CD11b$^+$CD115$^+$(%)	CD11b^{hi} (%)	CD11b^{lo} (%)
Wild-type	87.73±4.28	13.40±0.95	10.99±0.94	1.89±0.55
CCR1KO	91.75±2.33	9.67±0.43*	8.26±0.30*	0.63±0.09*
CX3CR1KO	91.93±1.53	14.35±1.90	13.00±1.98	1.01±0.02*

Population ratio of CD11b^{hi} (R1-gated) subpopulation and CD11b^{lo} (R2-gated) subpopulation of CD11b$^+$CD115$^+$ osteoclastic precursors (in Fig. 5) is shown as mean percentage ± s.e.m. (n=3). *Statistically significant (P<0.05), based on *post-hoc* test of one-factor factorial ANOVA.

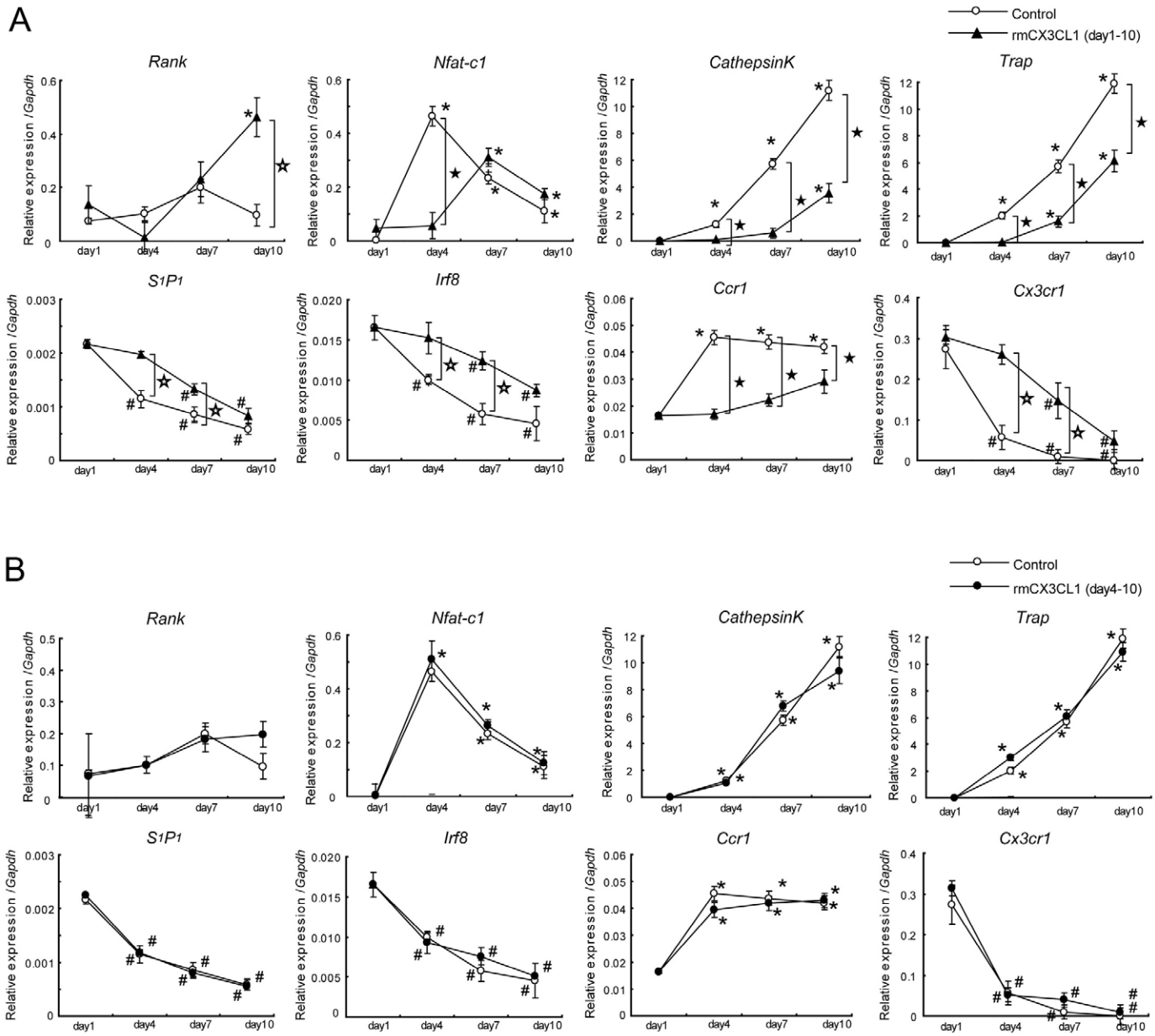

Fig. 8. Delay in osteoclastic marker expression after treatment with recombinant CX3CL1 prior to RANKL stimulation. The relative expression levels of transcripts of osteoclastic differentiation markers were measured using a RT-PCR analysis. The levels were normalized to the expression of *Gapdh*. Cells were cultured with M-CSF and RANKL for 10 days, stimulated with rmCX3CL1 (50 ng/ml) for days 1–10 (triangles), and for days 4–10 (filled circles), then were compared with unstimulated osteoclasts (open circles). *Significantly upregulated mRNA, and $^{\#}$significantly downregulated mRNA compared to the day 1 controls, P<0.05 (means ± s.e.m., n=3). The differences between unstimulated osteoclasts and rmCX3CL1-treated osteoclasts were significantly increased (☆P<0.05) and decreased (★P<0.05), respectively.

marrow environment, as previously reported by Koizumi et al. (Koizumi et al., 2009).

The osteoclastic phenotypes in CX3CR1 deficiency are very similar to those associated with CCR1 deficiency, which we reported in a previous study (Hoshino et al., 2010). In fact, the *Ccr1* expression was dramatically suppressed in *Cx3cr1*-deficient bones and was significantly reduced in *Cx3cr1*-deficient osteoclasts (Fig. 2E; Fig. 7B). However, some aspects of the osteoclast phenotypes in *Cx3cr1*-deficient cells exhibit distinct functions from those of the *Ccr1*-deficient osteoclasts. First, the *Cx3cr1*-deficient osteoclasts exhibited obvious actin ring formation, indicating that they have the ability to undergo cell fusion, which was not observed in the *Ccr1*-deficient cells (Hoshino et al., 2010). Second, the pit formation assay and zymography showed that *Cx3cr1*-deficient osteoclasts exert obvious mineral resorption abilities; however, the collagen digestion by *Cx3cr1*-deficient osteoclasts is partially abrogated (Fig. 6C,D), while *Ccr1*-deficient osteoclasts do not show obvious mineral resorption or collagen digestion (Hoshino et al., 2010).

A possible reason for these phenotypic differences between *Cx3cr1*- and *Ccr1*-deficient osteoclasts could be their distinct roles in osteoclastic precursors. A population analysis of the bone marrow cells in *Ccr1*-deficient mice after RANKL stimulation exhibited significant downregulation of $CD11b^{+}CD115^{+}$ osteoclastic precursors, while the same analysis of *Cx3cr1*-deficient mice showed a significant decrease only in the $CD11b^{lo}$ (R2 gated) subpopulation (Table 1).

Given the distinct temporal expression patterns and functions of CCR1 (Hoshino et al., 2010) and CX3CR1 in this work, the CCR1-mediated axis appears to function in a wider range of activities during the course of osteoclast differentiation than does the CX3CR1 axis. CCL5 and CCL9 are critical ligands for CCR1 in bone cells, and are activated in differentiated osteoclasts (Hoshino et al., 2010). Simultaneous blockade with neutralizing antibodies against CCL5 and CCL9 inhibited osteoclast formation to a comparable level to that by PTX treatment (Hoshino et al., 2010), therefore, it is likely that they are major chemokine ligands that transduce Gαi protein-mediated signals for osteoclastogenesis. In *Ccr1*-deficient osteoclasts, both *Ccl5* and *Ccl9* were significantly suppressed (Hoshino et al., 2010), while significant upregulation of *Ccl9* and partial reduction of *Ccr1* were observed in the corresponding *Cx3cr1*-deficient cells (Fig. 7B,C), which could lead a partial breakdown of the CCR1 axis during osteoclast differentiation and may cause a milder phenotype in terms of the osteoclast function in the *Cx3cr1*-deficient mice.

In conclusion, the present observations provide further evidence for the physiological roles of the CX3CR1–CX3CL1 axis in bone metabolism, including the functional differentiation of both osteoblasts and osteoclasts, through different modes of the CCR1-mediated axis. Our current findings emphasize the relevance of the CX3CR1–CX3CL1 axis as a therapeutic target for diseases associated with bone destruction, since this chemokine axis appears to play a pivotal role in the chemokine networks involved in bone metabolism. Further studies are needed to evaluate the potential of targeting this axis for therapy.

Materials and Methods

Mice

Standard C57BL/6 mice (6–9-week-old, male) were obtained from CLEA Japan. *Cx3cr1*-deficient mice (Niess et al., 2005) were purchased from Jackson laboratories and backcrossed for eight to ten generations on the C57BL/6 background. These mice were bred and maintained under pathogen-free conditions at the animal facilities of the University of Tokyo.

Laboratory animal care and experiments

All experiments were performed according to the Institutional Guidelines for the Care and Use of Laboratory Animals in Research and with the approval of the local ethics committees of the University of Tokyo, the Research Institute of International Medical Center of Japan and Tokyo Medical and Dental University.

Reagents

Recombinant murine M-CSF and RANKL were purchased from R&D Systems Inc. (Minneapolis, MN, USA) and PeproTech Inc. (Rocky Hill, NJ, USA), respectively. The recombinant soluble form of mouse CX3CL1/fractalkine (rmCX3CL1) was purchased from R&D Systems. Hamster anti-CX3CL1 neutralizing antibodies (anti-CX3CL1 neuAb) and control hamster IgG were provided by Dr Toshio Imai (Kan Research Institute, Kobe, Japan). Specific antibodies for murine CX3CR1 and CX3CL1 were purchased from Abcam (Cambridge, MA).

Peripheral quantitative computed tomography and microcomputed tomography

The bone scores were measured with peripheral Quantitative Computed Tomography (pQCT) using the XCT Research SA^{+} system (Stratec Medizintechnik GmbH, Pforzheim, Germany), as described previously (Hoshino et al., 2010). The scores were defined according to the American Society for Bone and Mineral Research standards (Hildebrand et al., 1999). The microstructure parameters were three-dimensionally calculated as described previously (Ito et al., 2005).

Bone histomorphometry

Bone histomorphometry was performerd as previously described (Hoshino et al., 2010). The nomenclature, symbols and units used in the present study are those recommended by the Nomenclature Committee of the American Society for Bone and Mineral Research (Parfitt et al., 1987).

Cell culture of bone-marrow-derived osteoclasts and osteoblastic cells

Murine bone marrow cells cultured in α-MEM were used as the sources of osteoclastic and osteoblastic cell cultures as previously described (Hoshino et al., 2010). In these cultures, the non-adherent cells were collected for bone-marrow-derived macrophages and osteoclastic cells, and adherent bone mesenchymal stromal cells were collected for osteoblastic cells. To generate pre-osteoclasts, non-adherent cells were passed through a column filled with Sephadex G-10 microspheres (Amersham Biosciences, Piscataway, NJ), and the cells were then cultured with 10 ng/ml M-CSF and 20 ng/ml RANKL for 4 days. The contamination of stromal/osteoblastic cells was monitored by an RT-PCR analysis, as a low expression level of the Osteoprotegerin gene indicates the presence of stromal/osteoblastic cells (Hoshino et al., 2010). For the differentiation analysis in the presence of rmCX3CL1, bone marrow cells were stimulated with M-CSF and RANKL (day 1 to day 10) in the presence or absence of rmCX3CL1 (50 ng/ml). The culture media were replaced every three days.

Osteoblastic differentiation in adherent bone marrow mesenchymal stromal cells was induced by culture in α-MEM containing osteogenic factors (10% FBS, 200 μM ascorbic acid, 10 mM β-glycerophosphate and 10 nM dexamethasone). The culture media was replaced once every 3 days. The mineral deposition was evaluated using von Kossa's method (Polysciences, Inc., Warrington, PA). The calcium content was quantified using the Calcium E-test from WAKO (Wako Chemicals, Osaka, Japan), and the results were normalized using the DNA content of the lysates.

Co-culture experiments with osteoclast precursors and osteoblasts were performed by inoculating bone-marrow-derived precursors (1×10^{5} cells/well) onto a layer of osteoblastic cells that had been cultured for 21 days with osteoblast-inducing media in 24-well plates as previously described (Hoshino et al., 2010). The bone resorption activity of the co-culture studies were also conducted using bone slices as described previously (Hoshino et al., 2010).

Immunohistochemical staining

Immunohistochemical staining of the tibiae dissected from 4-week-old C57BL/6 mice was conducted as previously described (Watanabe et al., 2012). Paraffin-embedded sections of 5 μm were stained with specific antibodies against CX3CR1 and CX3CL1 (Abcam, Cambridge, MA), followed by Alexa Fluor 568 antibodies (Molecular Probes, Life Technologies, Grand Island, NY), and were counterstained with DAPI (DOJINDO Laboratories, Kumamoto, Japan).

The osteoblastic cell line, MC3T3-E1 (RIKEN BOCC, Tsukuba, Japan), was maintained and cultured as previously described (Watanabe et al., 2012). Cells were seeded on 2-well culture slides (BD Falcon, San Jose, CA) and then fixed with 4% paraformaldehyde 2 and 4 days after culture. Double immunofluorescence staining was sequentially conducted using antibodies against CX3CR1 and

CX3CL1, and slides were counterstained with DAPI. Fluorescence images and differential interference contrast (DIC) images were captured using an ECLIPSE Ni-E fluorescence microscope (NIKON, Tokyo, Japan). Image processing was conducted using the NISE Elements software program (NIKON, Tokyo, Japan). Immunohistochemical staining of cultured osteoclasts were carried out as described previously (Hoshino et al., 2010).

Real-time quantitative PCR (RT-PCR) analysis

Total cellular RNA from the cultures of osteoclastic cells, osteoblastic cells and bone tissue sample (the proximal tibia after the removal of bone marrow at the metaphysial regions by flushing) was isolated using the RNeasy kit (Qiagen, Valencia, CA). The total RNA was then reverse-transcribed into cDNA using the Superscript III RT kit (Invitrogen, Carlsbad, CA). A real-time quantitative PCR (RT-PCR) analysis was performed using the ABI 7700 sequence detector system and the Taqman® Gene Expression Analysis software program (Applied Biosystems, Foster City, CA) as described previously (Hoshino et al., 2010).

Measurement of chemokines, TRAP, BALP and NTx

The murine chemokine levels were determined using ELISA for CCL5, MAB463 and BAF463 antibodies (R&D systems). Murine tartrate-resistant acid phosphatase 5b (TRAP5b), BALP and NTx in the serum and culture supernatants were measured using the murine TRAP EIA assay kit (Immunodiagnostic system, Fountain Hills, AZ), the murine BALP ELISA kit (Cusabio Biotech Co Ltd, Wilmington, DE) and the NTx ELISA kit (SRL, Inc., Tokyo, Japan), respectively.

Flow cytometry

Flow cytometric analysis of osteoclast precursors were performed as previously described (Hoshino et al., 2010). Pacific Blue-, FITC-, PE-, APC-, PerCP-Cy5.5-, PE-Cy7-, APC-Cy7 or biotin-conjugated anti-mouse antibodies to CD45.2 (104), CD115 (AFS98), CD265/RANK (R12-31) and subclass-matched control antibodies were purchased from eBioscience (San Diego, CA). Anti-mouse antibodies to FcγR (2.4G2), Ly6C/6G (RB6-8C5), CD11b (M1/70) and CD19 (1D3) were purchased from BD Pharmingen (San Diego, CA).

Statistical analyses

The data are presented as the means ± s.e.m. Statistical significance was determined with a *post-hoc* test or one-factor factorial ANOVA (Fig. 3C; Fig. 5; Fig. 7A–C; Table 1), Wilcoxon Mann–Whitney (non-parametric analysis, Fig. 2C), Tukey–Kramer HSD test (multiple comparisons, Fig. 3B–D and Fig. 8A,B) and Student's *t*-test (other figures) using the KaleidaGraph® 4.0 software program for Windows (Synergy Software, Reading, PA, USA). * and # indicate a significant upregulation and downregulation, respectively ($P<0.05$). NS: not significant.

Acknowledgements

The authors express sincere thanks to Mami Tamai, Satoshi Takiguchi and Norio Ohba at Nikon Instech., Ltd for their expertise on microscopy and image processing.

Funding

This work was supported by a Grant-in-Aid for Scientific Research from the Japan Society for the Promotion of Science [grant KAKENHI to A.H., A.Y. and T. Iimura]; the Naito Foundation to A.H.; the Ministry of Education, Culture, Sports, Science and Technology, Global Center of Excellence Program, 'International Research Center for Molecular Science in Tooth and Bone Diseases' to A.Y. and T. Iimura]; the Ministry of Education, Culture, Sports, Science and Technology Grant-in-Aid for Scientific Research on Innovative Areas 'Fluorescence Live Imaging' [grant number 22113002 to T. Iimura]; Takeda Science Foundation to T. Iimura; and the Ministry of Health, Labor and Welfare [grant number H19-nano-012 to K.Y.].

References

Arai, F., Miyamoto, T., Ohneda, O., Inada, T., Sudo, T., Brasel, K., Miyata, T., Anderson, D. M. and Suda, T. (1999). Commitment and differentiation of osteoclast precursor cells by the sequential expression of c-Fms and receptor activator of nuclear factor kappaB (RANK) receptors. *J. Exp. Med.* **190**, 1741-1754.

Bazan, J. F., Bacon, K. B., Hardiman, G., Wang, W., Soo, K., Rossi, D., Greaves, D. R., Zlotnik, A. and Schall, T. J. (1997). A new class of membrane-bound chemokine with a CX3C motif. *Nature* **385**, 640-644.

Binder, N. B., Niederreiter, B., Hoffmann, O., Stange, R., Pap, T., Stulnig, T. M., Mack, M., Erben, R. G., Smolen, J. S. and Redlich, K. (2009). Estrogen-dependent and C-C chemokine receptor-2-dependent pathways determine osteoclast behavior in osteoporosis. *Nat. Med.* **15**, 417-424.

Charo, I. F. and Ransohoff, R. M. (2006). The many roles of chemokines and chemokine receptors in inflammation. *N. Engl. J. Med.* **354**, 610-621.

Choi, S. J., Cruz, J. C., Craig, F., Chung, H., Devlin, R. D., Roodman, G. D. and Alsina, M. (2000). Macrophage inflammatory protein 1-alpha is a potential osteoclast stimulatory factor in multiple myeloma. *Blood* **96**, 671-675.

Degryse, B. and de Virgilio, M. (2003). The nuclear protein HMGB1, a new kind of chemokine? *FEBS Lett.* **553**, 11-17.

Delmas, P. D. (1993). Biochemical markers of bone turnover. *J. Bone Miner. Res.* **8 Suppl. 2**, S549-S555.

Ducy, P., Zhang, R., Geoffroy, V., Ridall, A. L. and Karsenty, G. (1997). Osf2/Cbfa1: a transcriptional activator of osteoblast differentiation. *Cell* **89**, 747-754.

Han, J. H., Choi, S. J., Kurihara, N., Koide, M., Oba, Y. and Roodman, G. D. (2001). Macrophage inflammatory protein-1alpha is an osteoclastogenic factor in myeloma that is independent of receptor activator of nuclear factor kappaB ligand. *Blood* **97**, 3349-3353.

Han, W., Ding, P., Xu, M., Wang, L., Rui, M., Shi, S., Liu, Y., Zheng, Y., Chen, Y., Yang, T. et al. (2003). Identification of eight genes encoding chemokine-like factor superfamily members 1-8 (CKLFSF1-8) by in silico cloning and experimental validation. *Genomics* **81**, 609-617.

Haringman, J. J., Smeets, T. J., Reinders-Blankert, P. and Tak, P. P. (2006). Chemokine and chemokine receptor expression in paired peripheral blood mononuclear cells and synovial tissue of patients with rheumatoid arthritis, osteoarthritis, and reactive arthritis. *Ann. Rheum. Dis.* **65**, 294-300.

Hildebrand, T., Laib, A., Müller, R., Dequeker, J. and Rüegsegger, P. (1999). Direct three-dimensional morphometric analysis of human cancellous bone: microstructural data from spine, femur, iliac crest, and calcaneus. *J. Bone Miner. Res.* **14**, 1167-1174.

Hoshino, A., Iimura, T., Ueha, S., Hanada, S., Maruoka, Y., Mayahara, M., Suzuki, K., Imai, T., Ito, M., Manome, Y. et al. (2010). Deficiency of chemokine receptor CCR1 causes osteopenia due to impaired functions of osteoclasts and osteoblasts. *J. Biol. Chem.* **285**, 28826-28837.

Imai, T., Hieshima, K., Haskell, C., Baba, M., Nagira, M., Nishimura, M., Kakizaki, M., Takagi, S., Nomiyama, H., Schall, T. J. et al. (1997). Identification and molecular characterization of fractalkine receptor CX3CR1, which mediates both leukocyte migration and adhesion. *Cell* **91**, 521-530.

Ishii, M., Egen, J. G., Klauschen, F., Meier-Schellersheim, M., Saeki, Y., Vacher, J., Proia, R. L. and Germain, R. N. (2009). Sphingosine-1-phosphate mobilizes osteoclast precursors and regulates bone homeostasis. *Nature* **458**, 524-528.

Ito, M., Ikeda, K., Nishiguchi, M., Shindo, H., Uetani, M., Hosoi, T. and Orimo, H. (2005). Multi-detector row CT imaging of vertebral microstructure for evaluation of fracture risk. *J. Bone Miner. Res.* **20**, 1828-1836.

Kanatani, N., Fujita, T., Fukuyama, R., Liu, W., Yoshida, C. A., Moriishi, T., Yamana, K., Miyazaki, T., Toyosawa, S. and Komori, T. (2006). Cbf beta regulates Runx2 function isoform-dependently in postnatal bone development. *Dev. Biol.* **296**, 48-61.

Kim, M. S., Magno, C. L., Day, C. J. and Morrison, N. A. (2006). Induction of chemokines and chemokine receptors CCR2b and CCR4 in authentic human osteoclasts differentiated with RANKL and osteoclast like cells differentiated by MCP-1 and RANTES. *J. Cell. Biochem.* **97**, 512-518.

Koizumi, K., Saitoh, Y., Minami, T., Takeno, N., Tsuneyama, K., Miyahara, T., Nakayama, T., Sakurai, H., Takano, Y., Nishimura, M. et al. (2009). Role of CX3CL1/fractalkine in osteoclast differentiation and bone resorption. *J. Immunol.* **183**, 7825-7831.

Komori, T., Yagi, H., Nomura, S., Yamaguchi, A., Sasaki, K., Deguchi, K., Shimizu, Y., Bronson, R. T., Gao, Y. H., Inada, M. et al. (1997). Targeted disruption of Cbfa1 results in a complete lack of bone formation owing to maturational arrest of osteoblasts. *Cell* **89**, 755-764.

Li, X., Qin, L., Bergenstock, M., Bevelock, L. M., Novack, D. V. and Partridge, N. C. (2007). Parathyroid hormone stimulates osteoblastic expression of MCP-1 to recruit and increase the fusion of pre/osteoclasts. *J. Biol. Chem.* **282**, 33098-33106.

Liu, W., Toyosawa, S., Furuichi, T., Kanatani, N., Yoshida, C., Liu, Y., Himeno, M., Narai, S., Yamaguchi, A. and Komori, T. (2001). Overexpression of Cbfa1 in osteoblasts inhibits osteoblast maturation and causes osteopenia with multiple fractures. *J. Cell Biol.* **155**, 157-166.

Ludwig, A. and Mentlein, R. (2008). Glial cross-talk by transmembrane chemokines CX3CL1 and CXCL16. *J. Neuroimmunol.* **198**, 92-97.

Menu, E., De Leenheer, E., De Raeve, H., Coulton, L., Imanishi, T., Miyashita, K., Van Valckenborgh, E., Van Riet, I., Van Camp, B., Horuk, R. et al. (2006). Role of CCR1 and CCR5 in homing and growth of multiple myeloma and in the development of osteolytic lesions: a study in the 5TMM model. *Clin. Exp. Metastasis* **23**, 291-300.

Nakashima, K., Zhou, X., Kunkel, G., Zhang, Z., Deng, J. M., Behringer, R. R. and de Crombrugghe, B. (2002). The novel zinc finger-containing transcription factor osterix is required for osteoblast differentiation and bone formation. *Cell* **108**, 17-29.

Niess, J. H., Brand, S., Gu, X., Landsman, L., Jung, S., McCormick, B. A., Vyas, J. M., Boes, M., Ploegh, H. L., Fox, J. G. et al. (2005). CX3CR1-mediated dendritic cell access to the intestinal lumen and bacterial clearance. *Science* **307**, 254-258.

Noels, H., Bernhagen, J. and Weber, C. (2009). Macrophage migration inhibitory factor: a noncanonical chemokine important in atherosclerosis. *Trends Cardiovasc. Med.* **19**, 76-86.

Oba, Y., Lee, J. W., Ehrlich, L. A., Chung, H. Y., Jelinek, D. F., Callander, N. S., Horuk, R., Choi, S. J. and Roodman, G. D. (2005). MIP-1alpha utilizes both CCR1

and CCR5 to induce osteoclast formation and increase adhesion of myeloma cells to marrow stromal cells. *Exp. Hematol.* **33**, 272-278.

Parfitt, A. M., Drezner, M. K., Glorieux, F. H., Kanis, J. A., Malluche, H., Meunier, P. J., Ott, S. M., Recker, R. R.; Report of the ASBMR Histomorphometry Nomenclature Committee (1987). Bone histomorphometry: standardization of nomenclature, symbols, and units. *J. Bone Miner. Res.* **2**, 595-610.

Saitoh, Y., Koizumi, K., Sakurai, H., Minami, T. and Saiki, I. (2007). RANKL-induced down-regulation of CX3CR1 via PI3K/Akt signaling pathway suppresses Fractalkine/CX3CL1-induced cellular responses in RAW264.7 cells. *Biochem. Biophys. Res. Commun.* **364**, 417-422.

Schneider, D. L. and Barrett-Connor, E. L. (1997). Urinary N-telopeptide levels discriminate normal, osteopenic, and osteoporotic bone mineral density. *Arch. Intern. Med.* **157**, 1241-1245.

Sheikine, Y. and Sirsjö, A. (2008). CXCL16/SR-PSOX—a friend or a foe in atherosclerosis? *Atherosclerosis* **197**, 487-495.

Shimaoka, T., Nakayama, T., Fukumoto, N., Kume, N., Takahashi, S., Yamaguchi, J., Minami, M., Hayashida, K., Kita, T., Ohsumi, J. et al. (2004). Cell surface-anchored SR-PSOX/CXC chemokine ligand 16 mediates firm adhesion of CXC chemokine receptor 6-expressing cells. *J. Leukoc. Biol.* **75**, 267-274.

Shimaoka, T., Seino, K., Kume, N., Minami, M., Nishime, C., Suematsu, M., Kita, T., Taniguchi, M., Matsushima, K. and Yonehara, S. (2007). Critical role for CXC chemokine ligand 16 (SR-PSOX) in Th1 response mediated by NKT cells. *J. Immunol.* **179**, 8172-8179.

Takahashi, M., Kushida, K., Hoshino, H., Ohishi, T. and Inoue, T. (1997). Evaluation of bone turnover in postmenopause, vertebral fracture, and hip fracture using biochemical markers for bone formation and resorption. *J. Endocrinol. Invest.* **20**, 112-117.

Wang, Y., Zhang, Y., Yang, X., Han, W., Liu, Y., Xu, Q., Zhao, R., Di, C., Song, Q. and Ma, D. (2006). Chemokine-like factor 1 is a functional ligand for CC chemokine receptor 4 (CCR4). *Life Sci.* **78**, 614-621.

Watanabe, T., Tamamura, Y., Hoshino, A., Makino, Y., Kamioka, H., Amagasa, T., Yamaguchi, A. and Iimura, T. (2012). Increasing participation of sclerostin in postnatal bone development, revealed by three-dimensional immunofluorescence morphometry. *Bone* **51**, 447-458.

Yang, M., Mailhot, G., MacKay, C. A., Mason-Savas, A., Aubin, J. and Odgren, P. R. (2006). Chemokine and chemokine receptor expression during colony stimulating factor-1-induced osteoclast differentiation in the toothless osteopetrotic rat: a key role for CCL9 (MIP-1gamma) in osteoclastogenesis in vivo and in vitro. *Blood* **107**, 2262-2270.

Yoshida, C. A., Komori, H., Maruyama, Z., Miyazaki, T., Kawasaki, K., Furuichi, T., Fukuyama, R., Mori, M., Yamana, K., Nakamura, K. et al. (2012). SP7 inhibits osteoblast differentiation at a late stage in mice. *PLoS ONE* **7**, e32364.

Zhao, B., Takami, M., Yamada, A., Wang, X., Koga, T., Hu, X., Tamura, T., Ozato, K., Choi, Y., Ivashkiv, L. B. et al. (2009). Interferon regulatory factor-8 regulates bone metabolism by suppressing osteoclastogenesis. *Nat. Med.* **15**, 1066-1071.